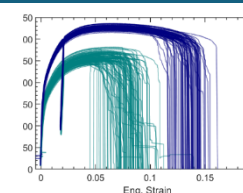
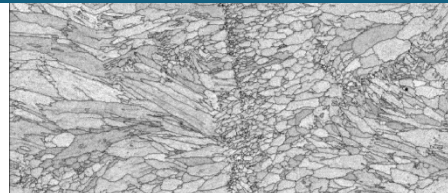
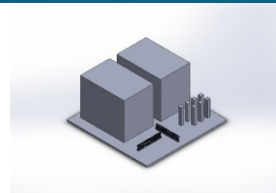




Sandia
National
Laboratories

The Influence of Regional Mechanics and Surface Defects on AM Al-Si10-Mg



Thomas A. Ivanoff, Nathan M. Heckman, Andrew T. Polonsky, and Kyle L. Johnson

SEM 2022 Annual Meeting and Exhibition
June 13th, 2022
Submission #: 13665



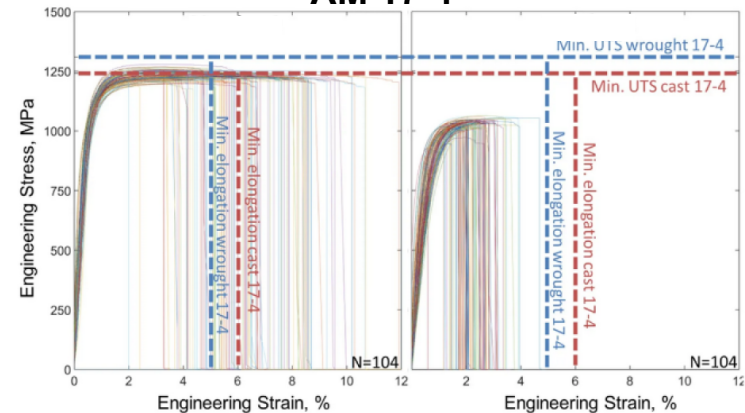
Sandia National Laboratories is a multimission laboratory managed and operated by National Technology & Engineering Solutions of Sandia, LLC, a wholly owned subsidiary of Honeywell International Inc., for the U.S. Department of Energy's National Nuclear Security Administration under contract DE-NA0003525.

2 Motivation and Goals



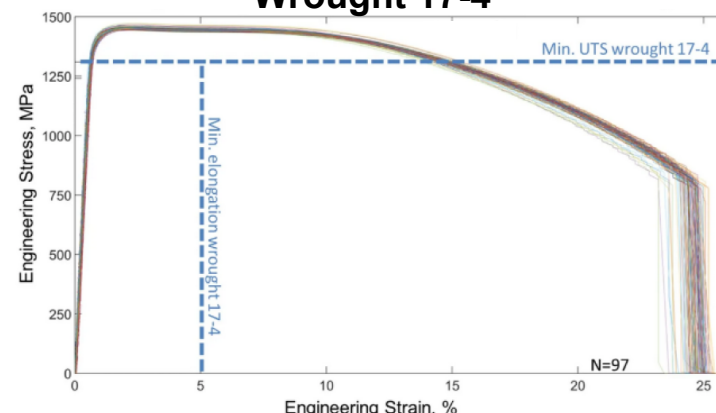
1. Previous work demonstrated variability in AM performance

AM 17-4



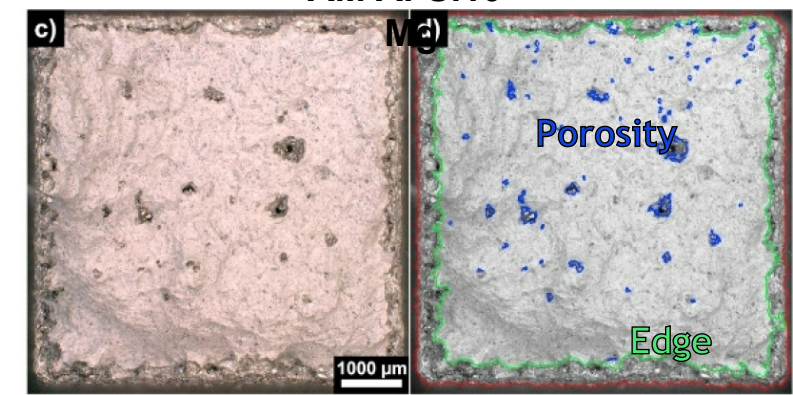
Salzbrenner, B.C. et al. J. Mat. Proc. Tech., 2017

Wrought 17-4



2. Edge effects lead to stochasticity

AM Al-Si10-

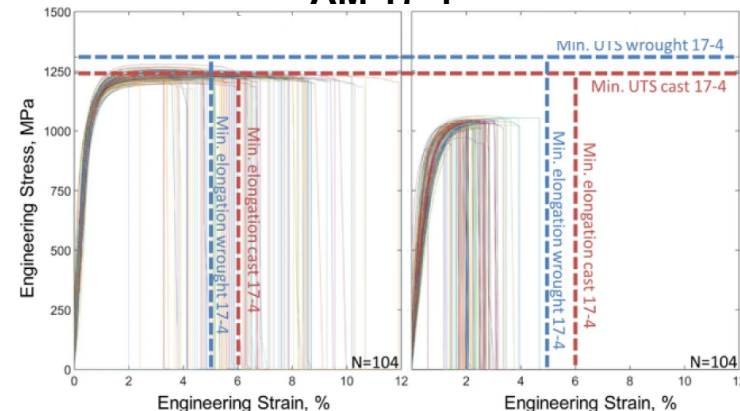


Motivation and Goals



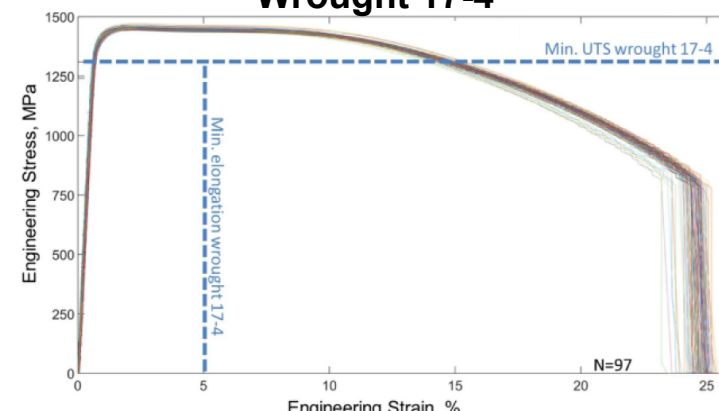
1. Previous work demonstrated variability in AM performance

AM 17-4



Salzbrenner, B.C. et al. J. Mat. Proc. Tech., 2017

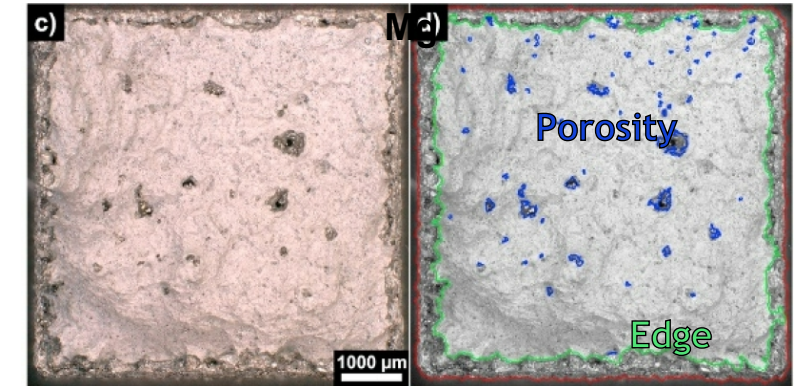
Wrought 17-4



2. Edge effects lead to stochasticity

AM Al-Si10-

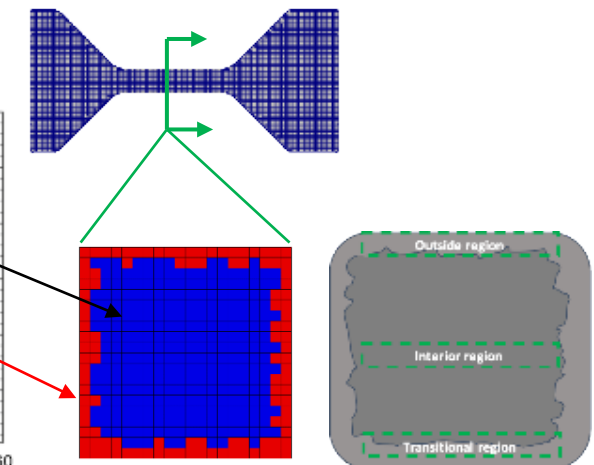
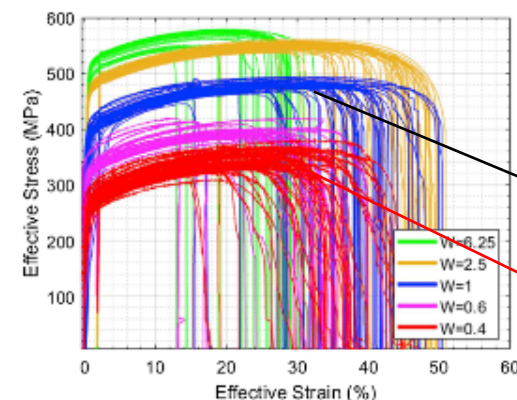
Mc



Laursen, C.M. et al. Mat. Sci. Eng. A, 2020

1. Characterize local behavior in AM metals

2. Develop experimentally-informed modeling/meshing solutions to aid AM metals design and qualification

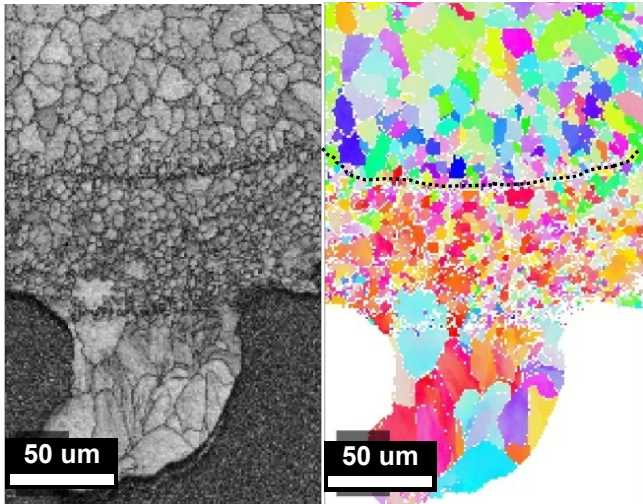


Roach, A.M. et al., Additive Manufacturing 2020

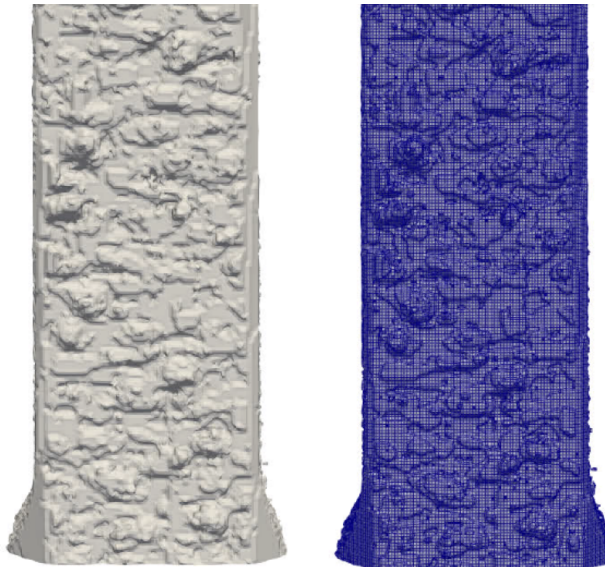
Project Workflow



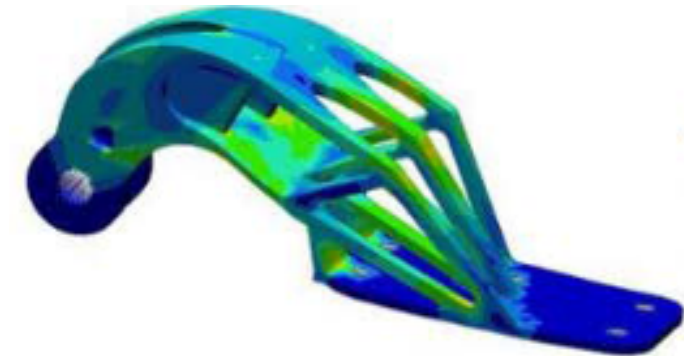
Current Status



Short Term



Long Term



Gebria, A.W. et al. IOP Conf. Ser: Mater. Sci. Eng., 2017

- Identify dominating edge/local mechanics in AM metals
- Identify distinguishing features of different regions in AM metals

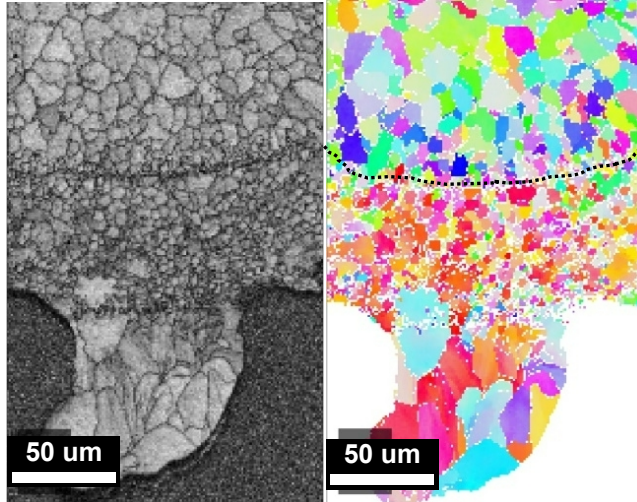
- Incorporate mechanics into high fidelity models
- Validate response in complex geometries

- Reduced fidelity modeling
- First-pass mod/sim technology
- Quantify uncertainty

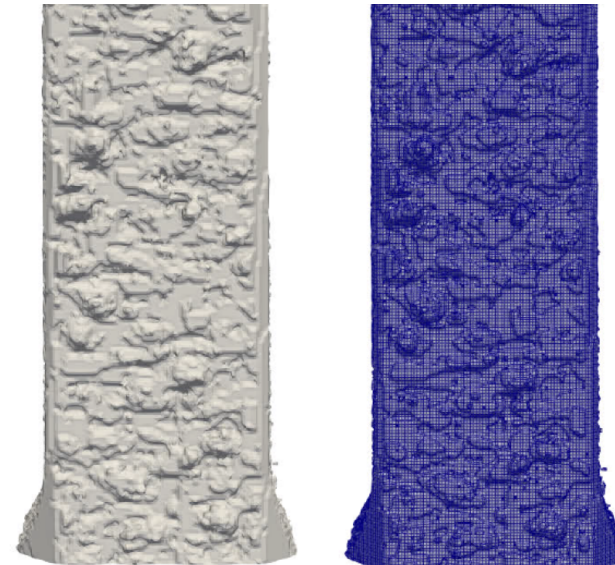
Project Workflow



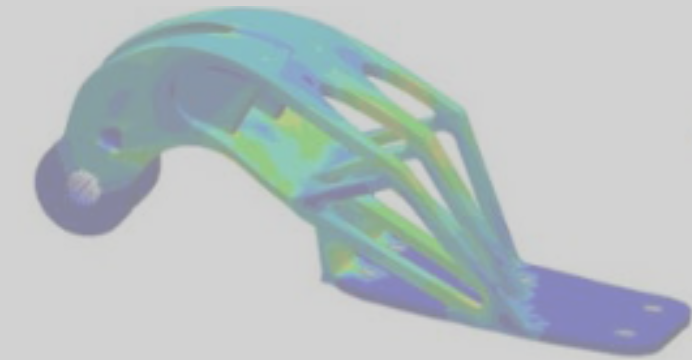
Current Status



Short Term



Long Term



Gebisa, A.W. et al. IOP Conf. Ser: Mater. Sci. Eng., 2017

- Identify dominating edge/local mechanics in AM metals
- Identify distinguishing features of different regions in AM metals

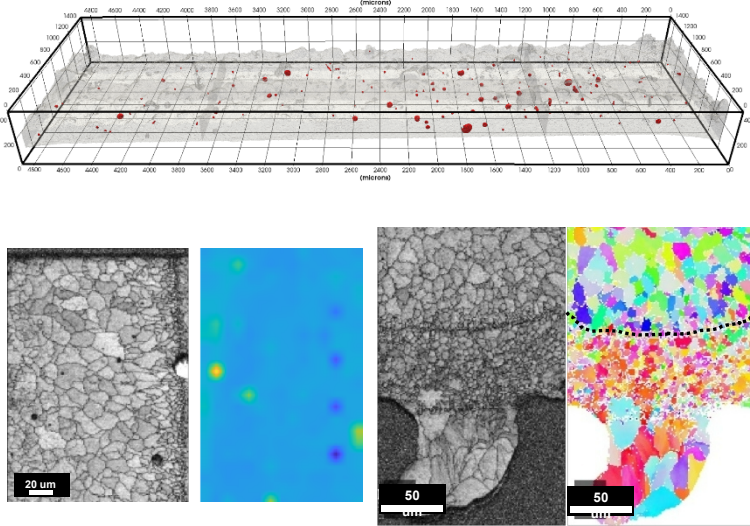
- Incorporate mechanics into high fidelity models
- Validate response in complex geometries

- Reduced fidelity modeling
- First-pass mod/sim technology
- Quantify uncertainty

6 Experimental Methods

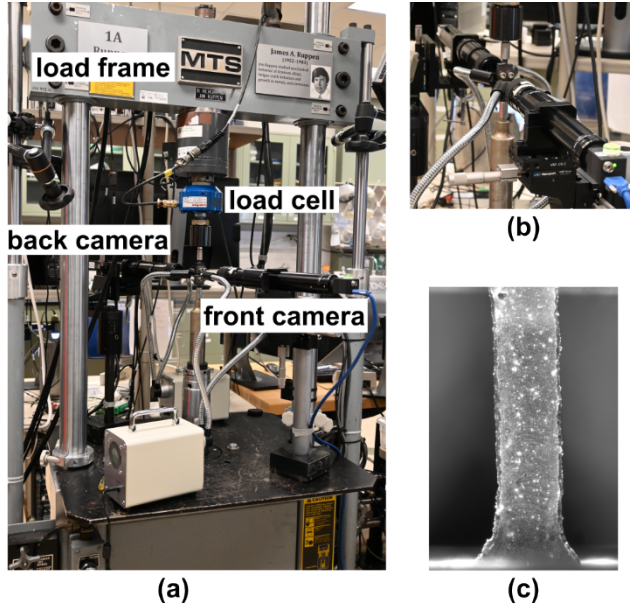


Characterization



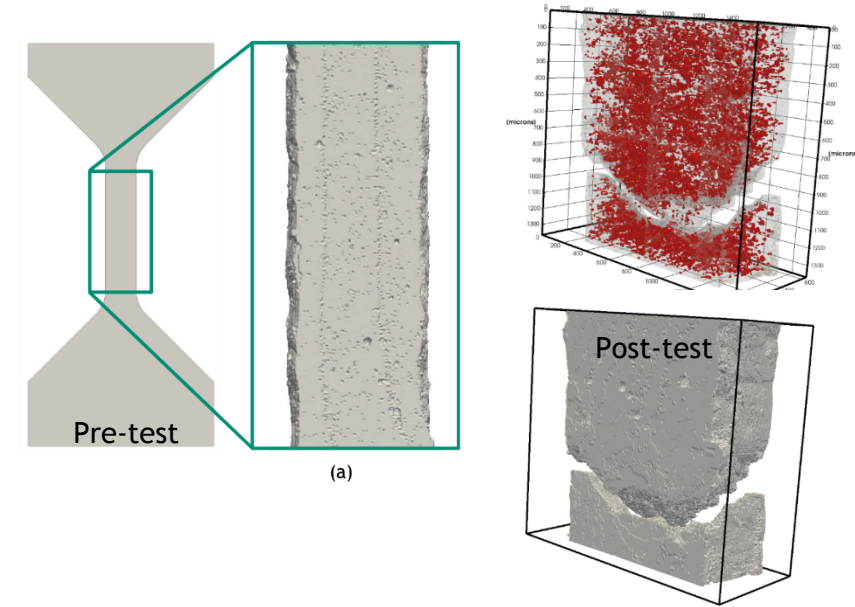
- Identify microstructural features that impact local response (e.g. grain structure and porosity)
- Electron microscopy, micro-computed tomography, nano-indentation

Mechanical Testing



- Determine strength/ductility discrepancies between the surface and interior
- In-situ DIC and micro-computed tomography tensile testing

High-fidelity modeling

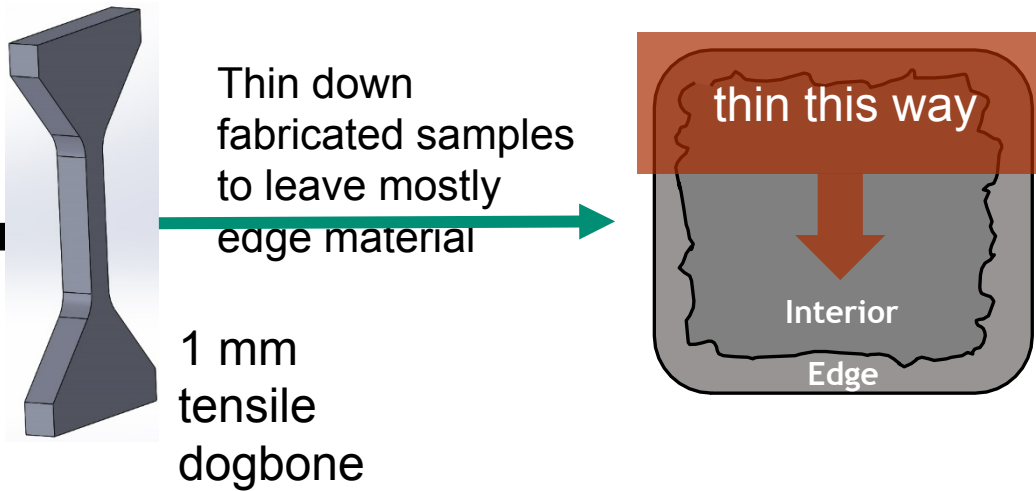


- Determine strength/ductility differences between the surface and interior
- In-situ DIC and micro-computed tomography

Experimental Methods



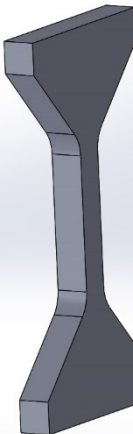
How do we isolate the edge region for mechanical testing?



Experimental Methods

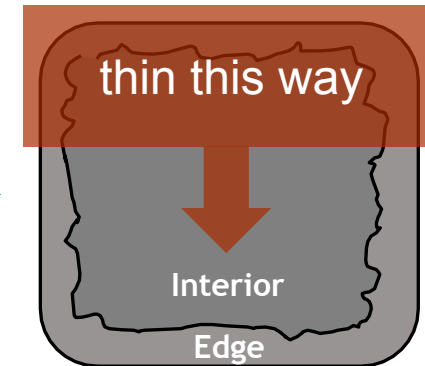


How do we isolate the edge region for mechanical testing?

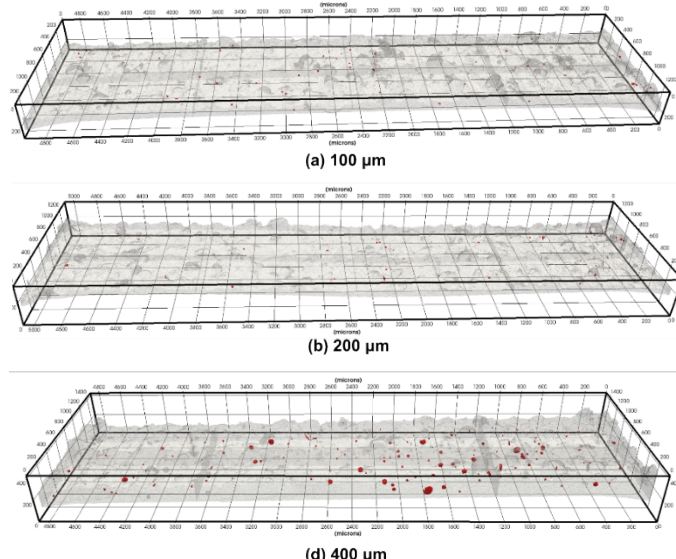
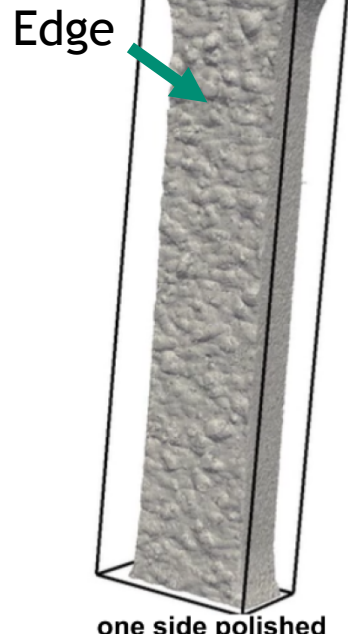


Thin down
fabricated samples
to leave mostly
edge material

1 mm
tensile
dogbone

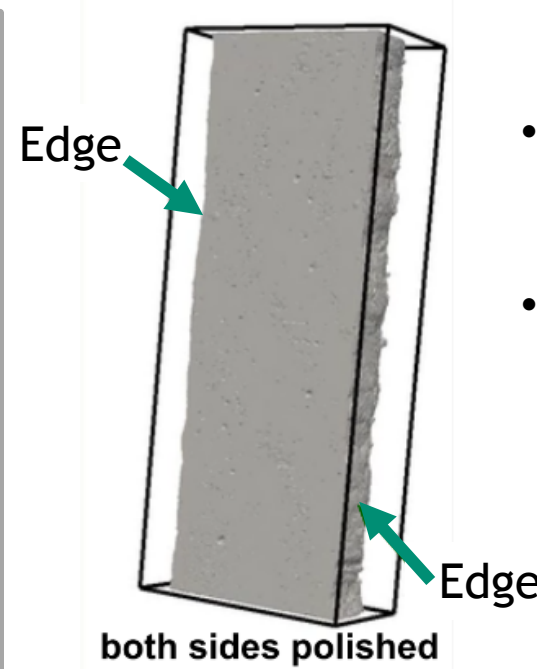


One-sided Thinning



- different thicknesses to vary edge/interior ratio

Two-sided Thinning



- Thinned to ~500 μm thick
- Edge only on sides of dogbone; allows in-situ observation of failure progression

9 AM Al-Si10-Mg Material

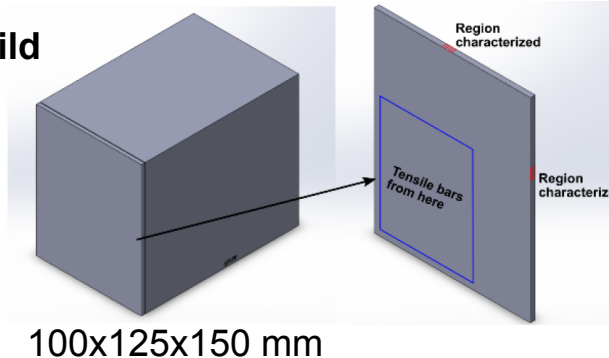


Laser Powder Bed Fusion (LPBF) Al-Si10-Mg from 2 vendors

- Different tools but nominally equivalent powder
- 1 mm tensile dogbones EDM cut from large builds
- Compare large and small
- Compare across vendors

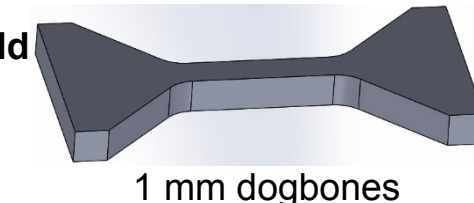
Vendor 1

Large Build



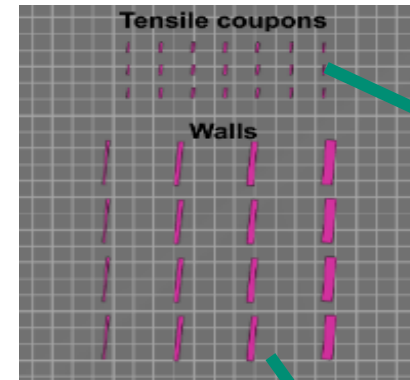
- 1 mm dogbones EDM cut from the large build
- One-sided thinned

Small Build



- Two-sided thinned

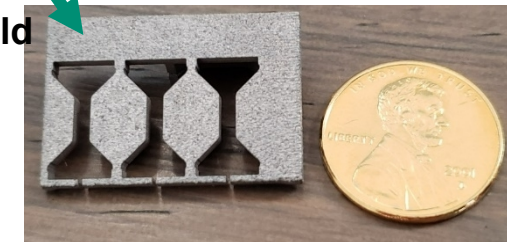
Vendor 2



Small Build

- Two-sided thinned

Large Build

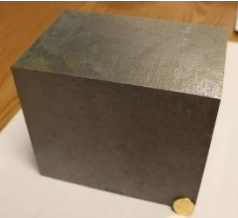


- 1 mm dogbones EDM cut from the larger walls
- One-sided thinned

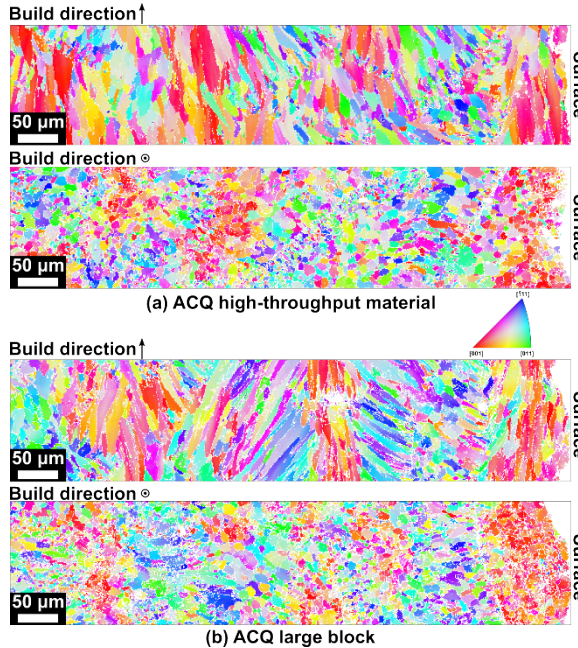
Microstructure



1 mm
dogbone

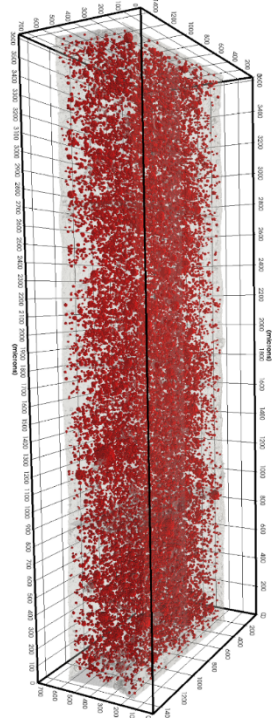
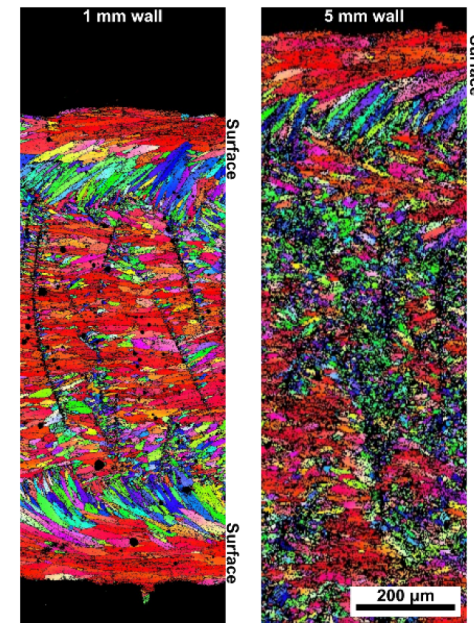


Vendor 1



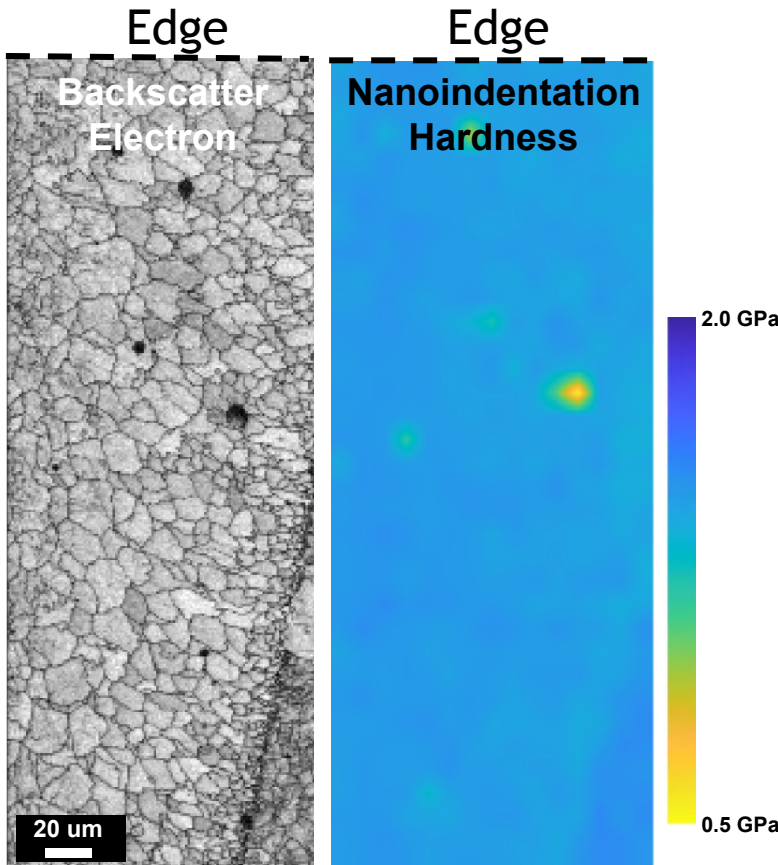
<1% porosity

Vendor 2

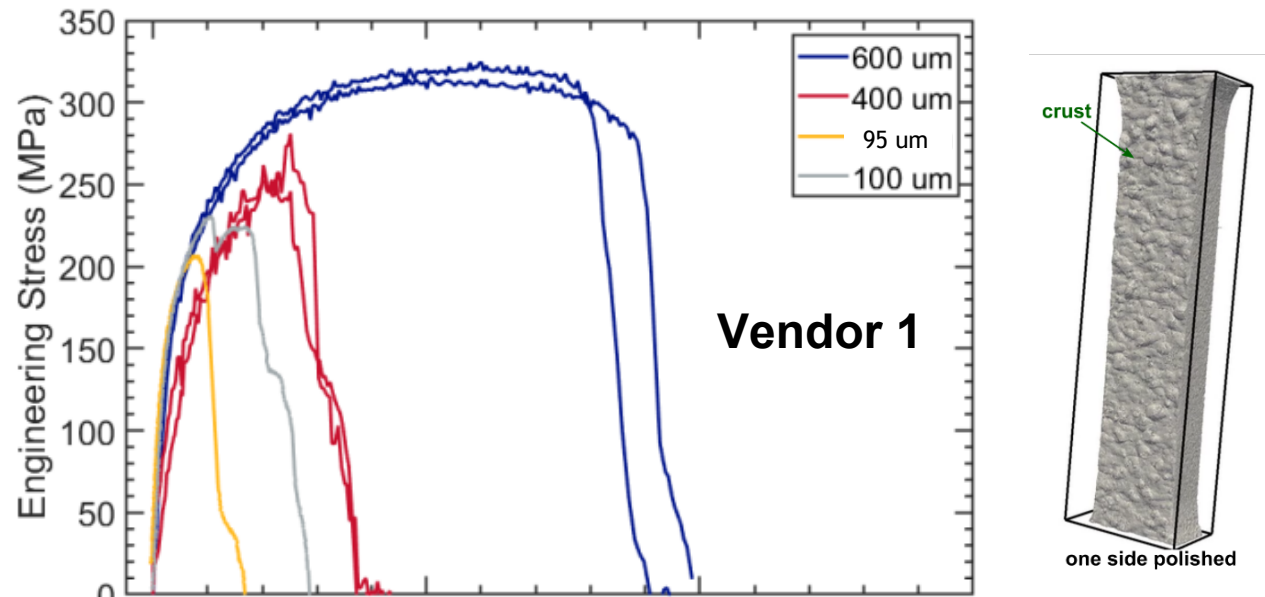


- Variation in grain size and texture along the edge of both materials
- Porosity content from CT scans significantly different between vendors
 - Note: 3D reconstruction can deceptively represent pore content

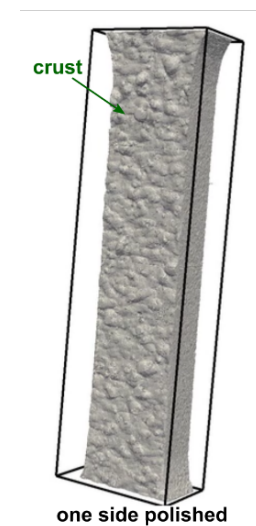
Mechanical Response



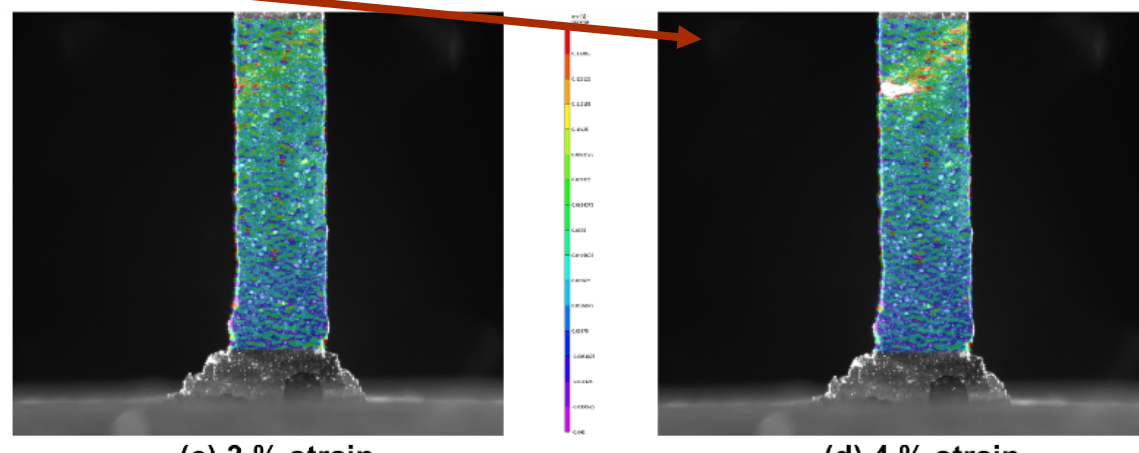
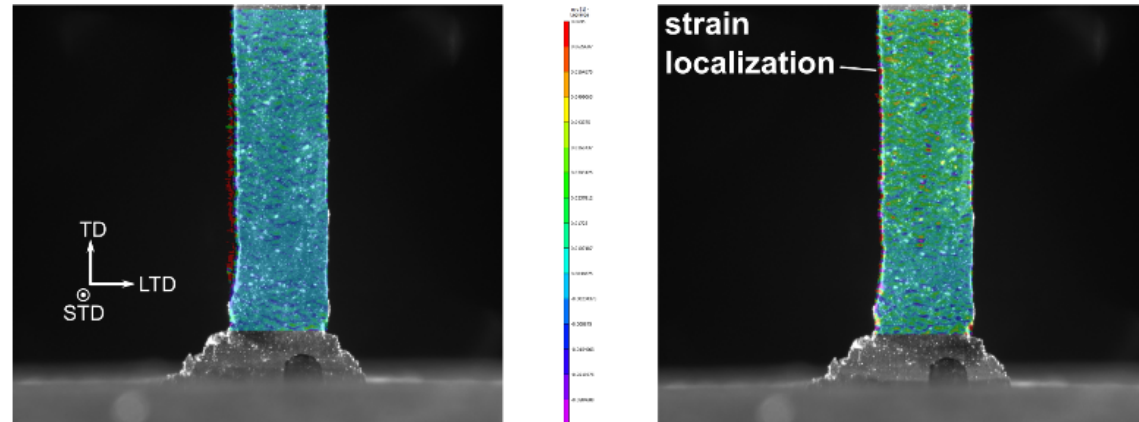
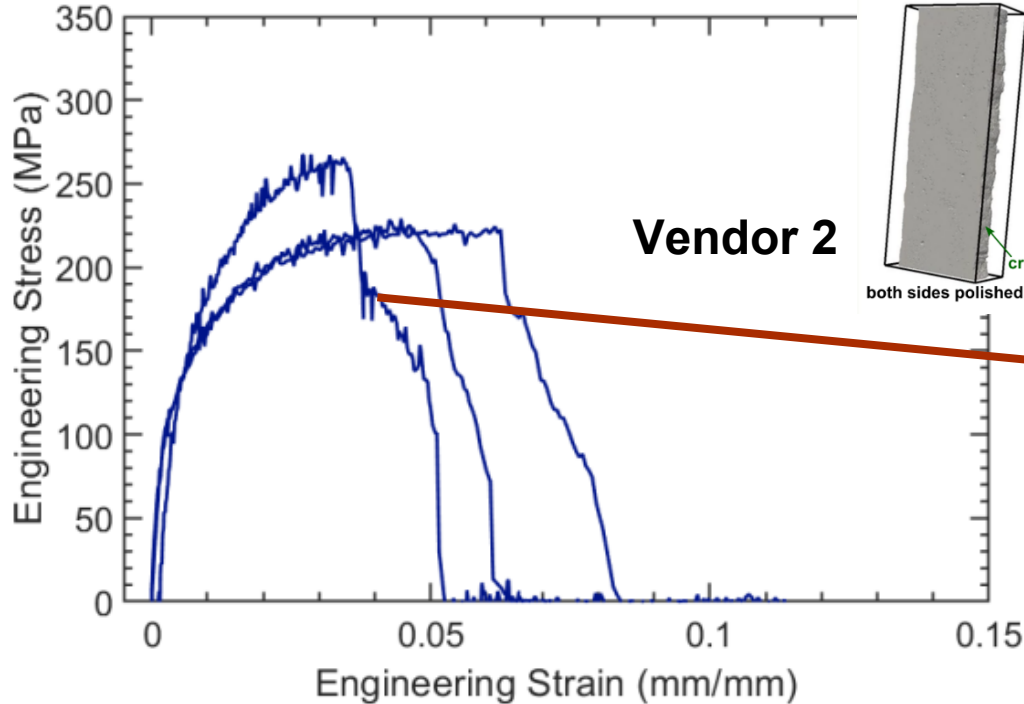
- Nano-indentation did not reveal gradients in local strength from edge to interior material



- Similar stress-strain responses with common elastic behavior
- Ductility decreases significantly with decreasing thickness
- UTS, ductility, and yield strength strong functions of thickness; suggest that edge material behaves differently than the interior
- Reduced performance is likely attributed to surface defects and texture variation in the edge material increasing damage



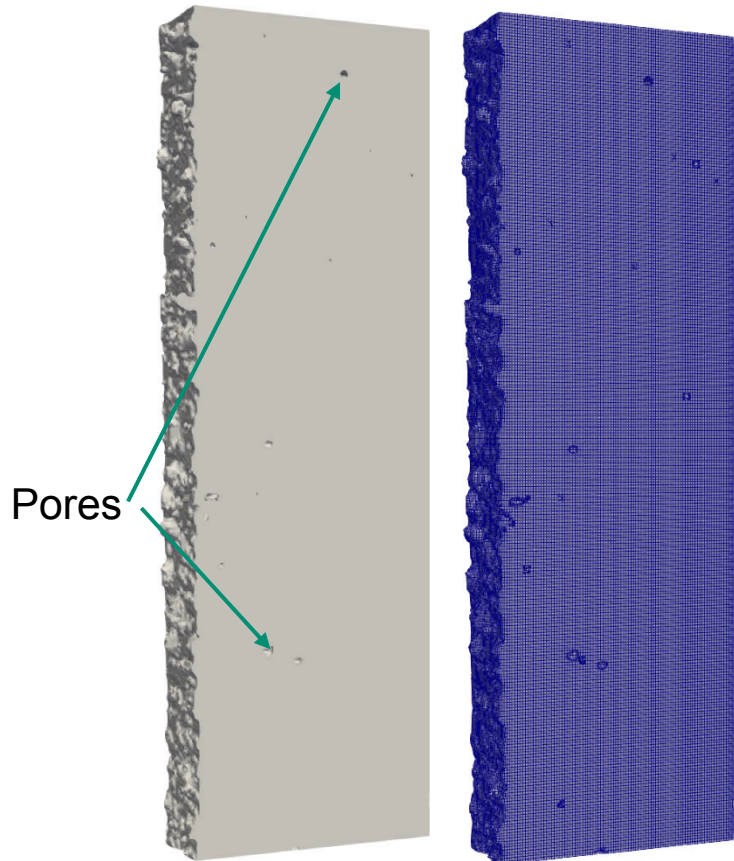
Mechanical Response



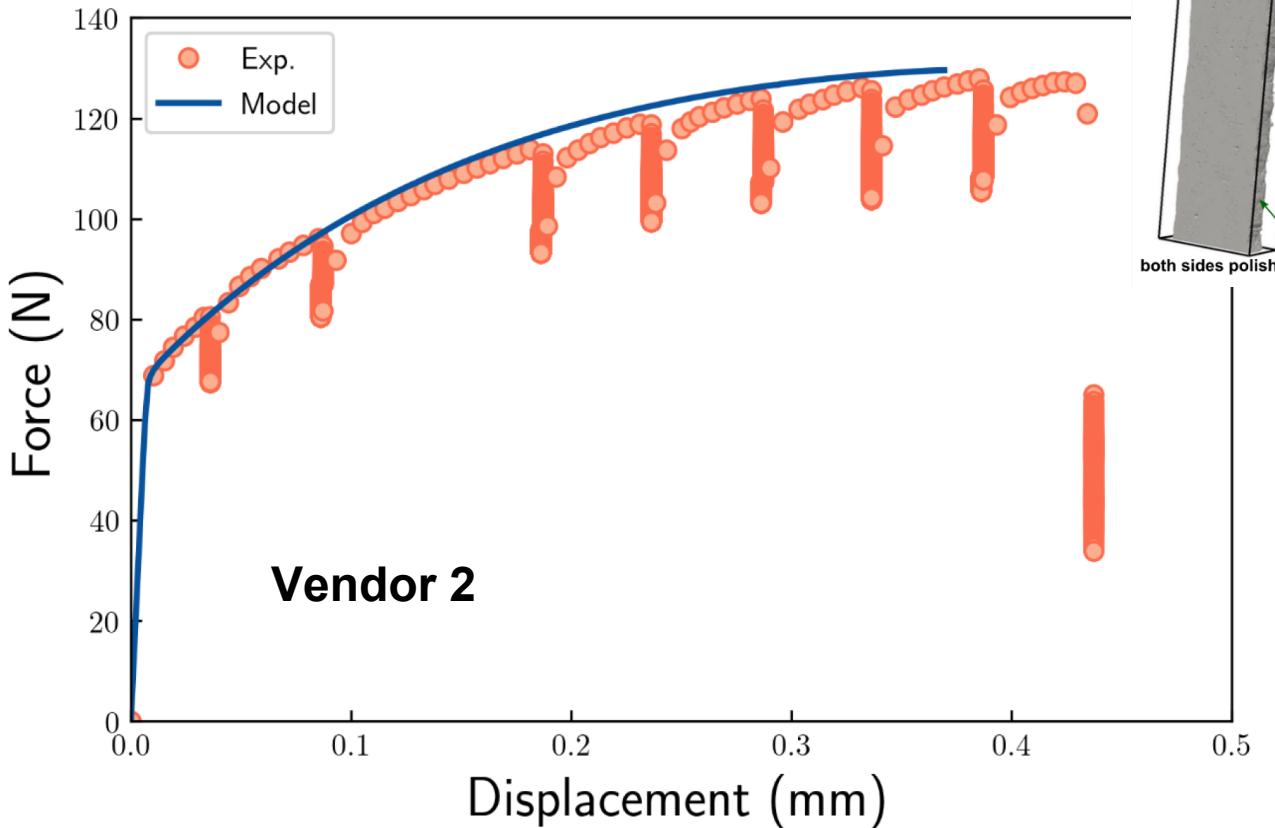
- Stress-strain response similar to the specimens thinned from one side
- Variability between tests from differences in thickness

- DIC highlights strain localization along the edge material and formation of a elevated strain band
- Failure spreads from the exterior and across the sample along a path of high strain

High-fidelity Modeling of In-situ Test

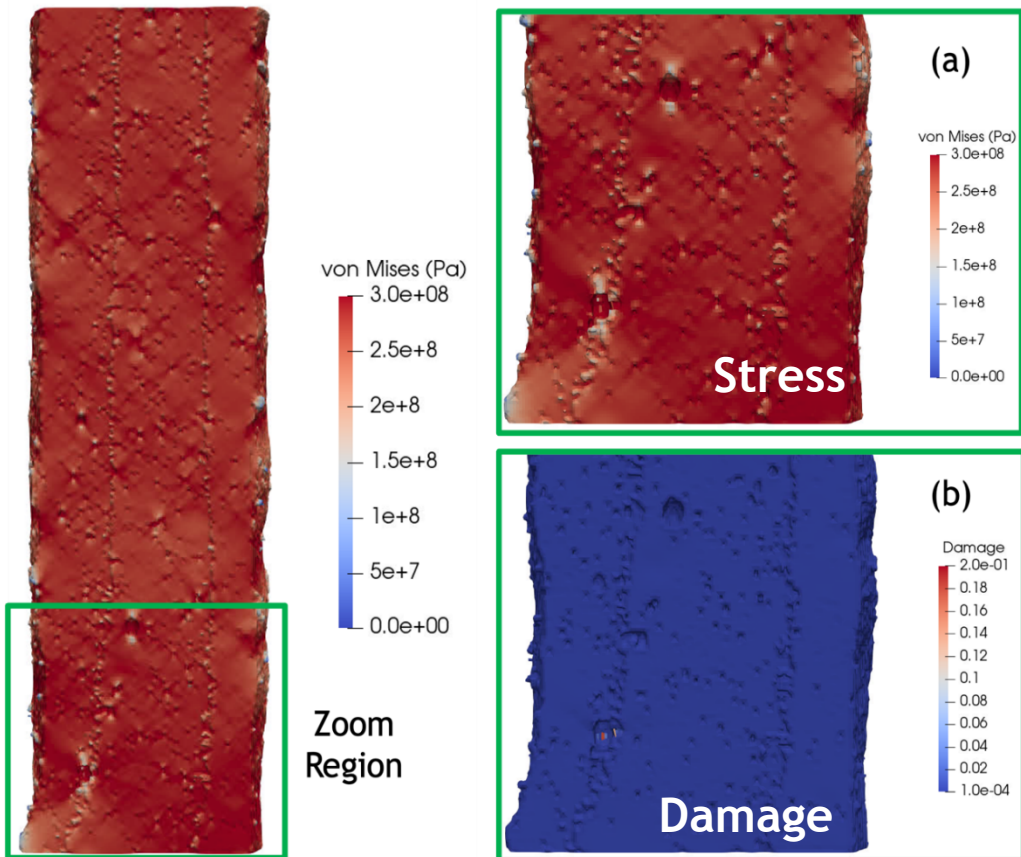


- CT scan directly used to mesh geometry
- Direct numerical simulations (DNS) of these meshes paired with in situ tensile testing allows for comparison of edge, geometry, and pore effects



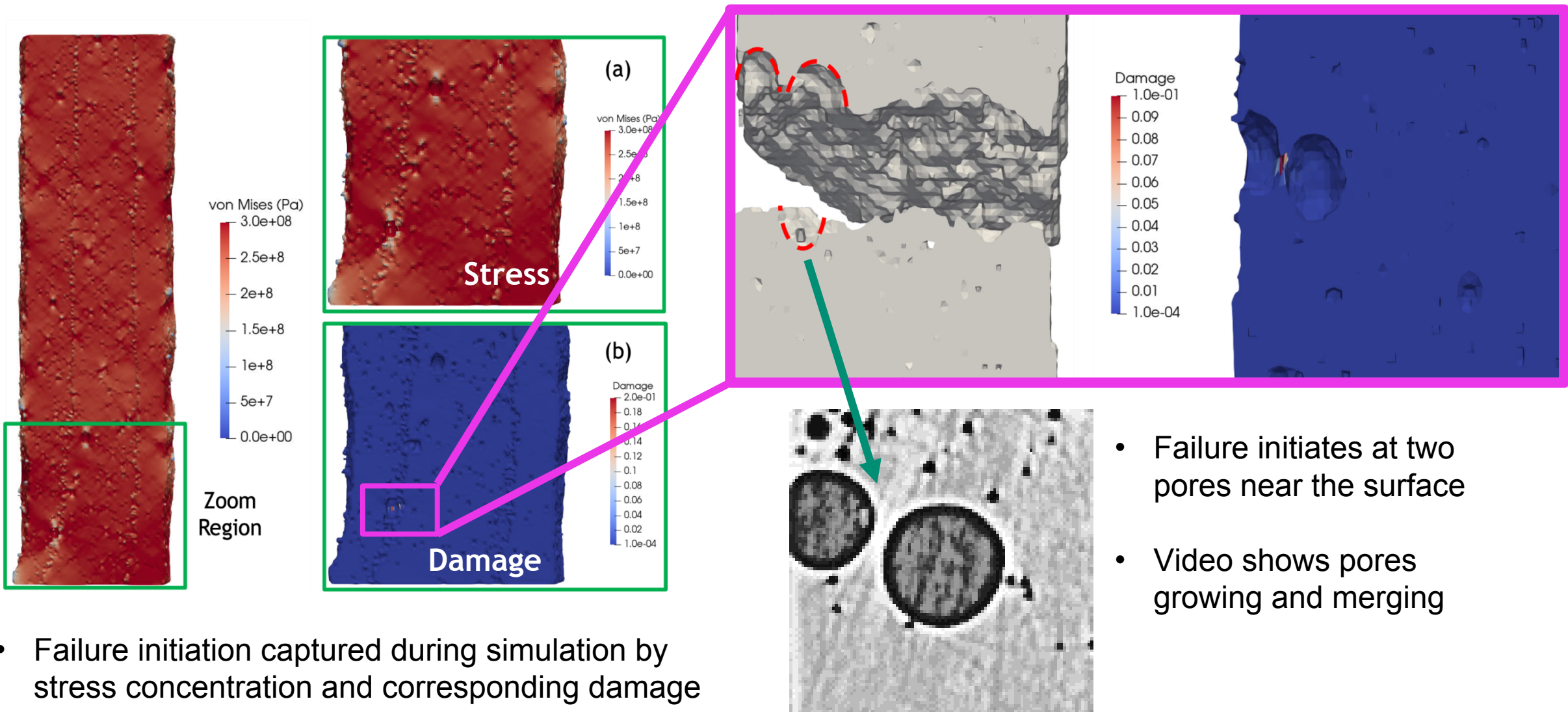
- Predictions for force-displacement follow experimental results
- Plasticity captured accurately with high-fidelity meshing of geometry

High-fidelity Modeling of In-situ Test



- Failure initiation captured during simulation by stress concentration and corresponding damage accumulation

High-fidelity Modeling of In-situ Test



Summary

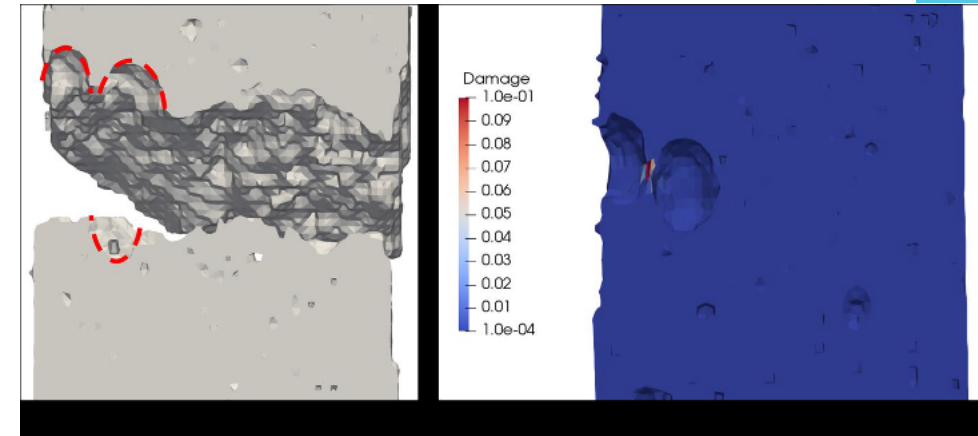


Key results

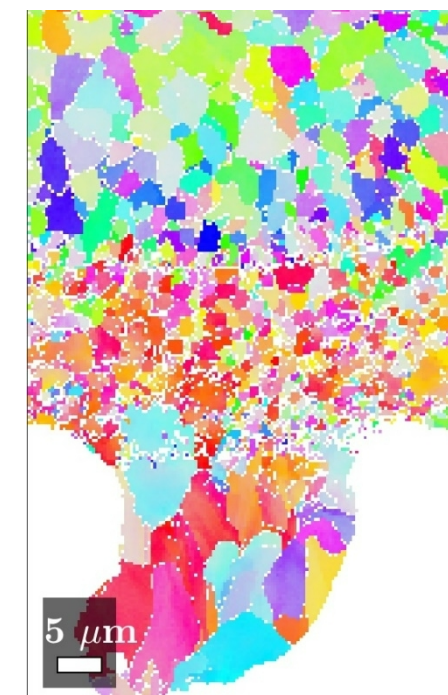
- Grain structure along edges contributes to variability in AM
- Local strength gradients not present as a source of variability
- Geometry and surface asperities exert an outsized role in determining failure initiation and progression
- Predicted localized response in AM Al-10Si-Mg using high-fidelity characterizations

Next steps and challenges

- Securing funding for long-term objectives
- Perform experiments on complex geometries
- Explore whether these observations are consistent in other alloys
- Does edge behavior have similar impact for fatigue loading?



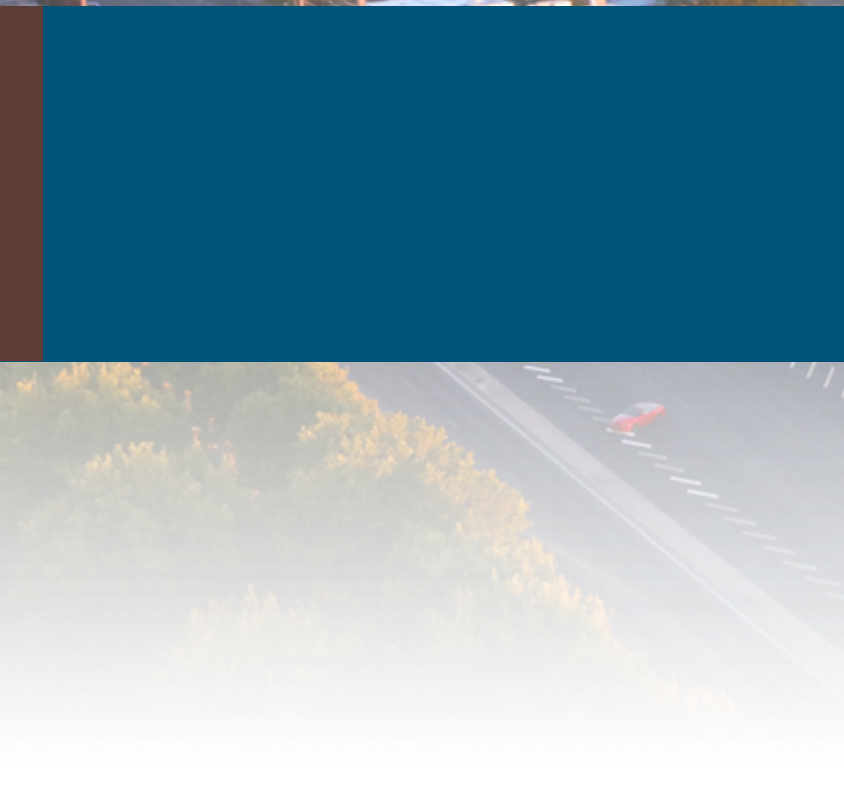
Strain and failure localization along the edge was correctly predicted from high-fidelity modeling



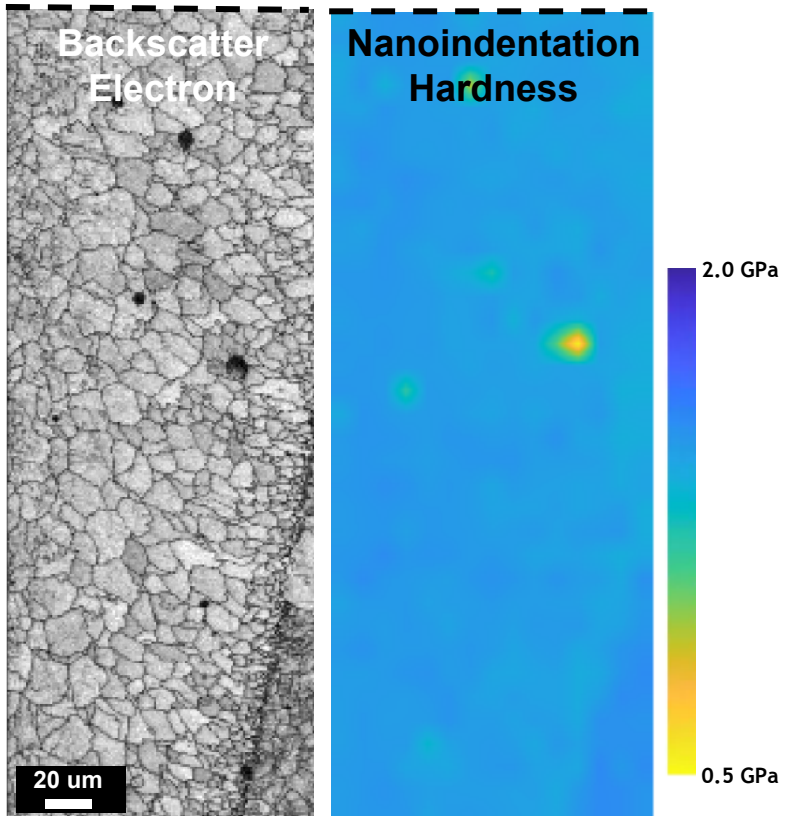
Grain structure variation along the edge of AM Al-10Si-Mg



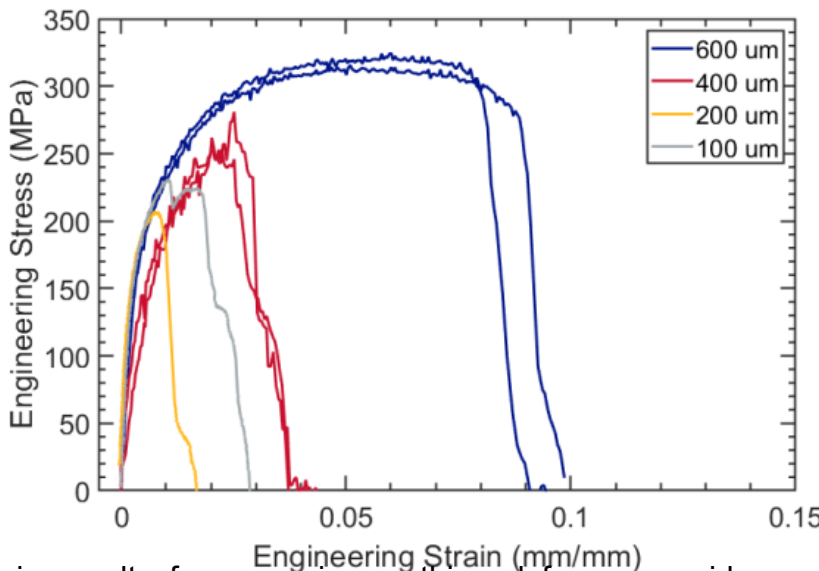
Backup Slides



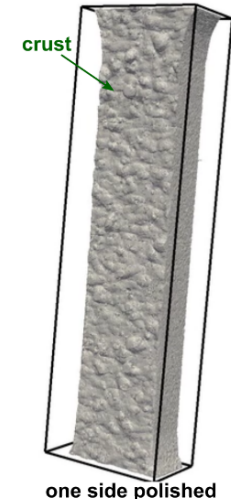
Mechanical Response



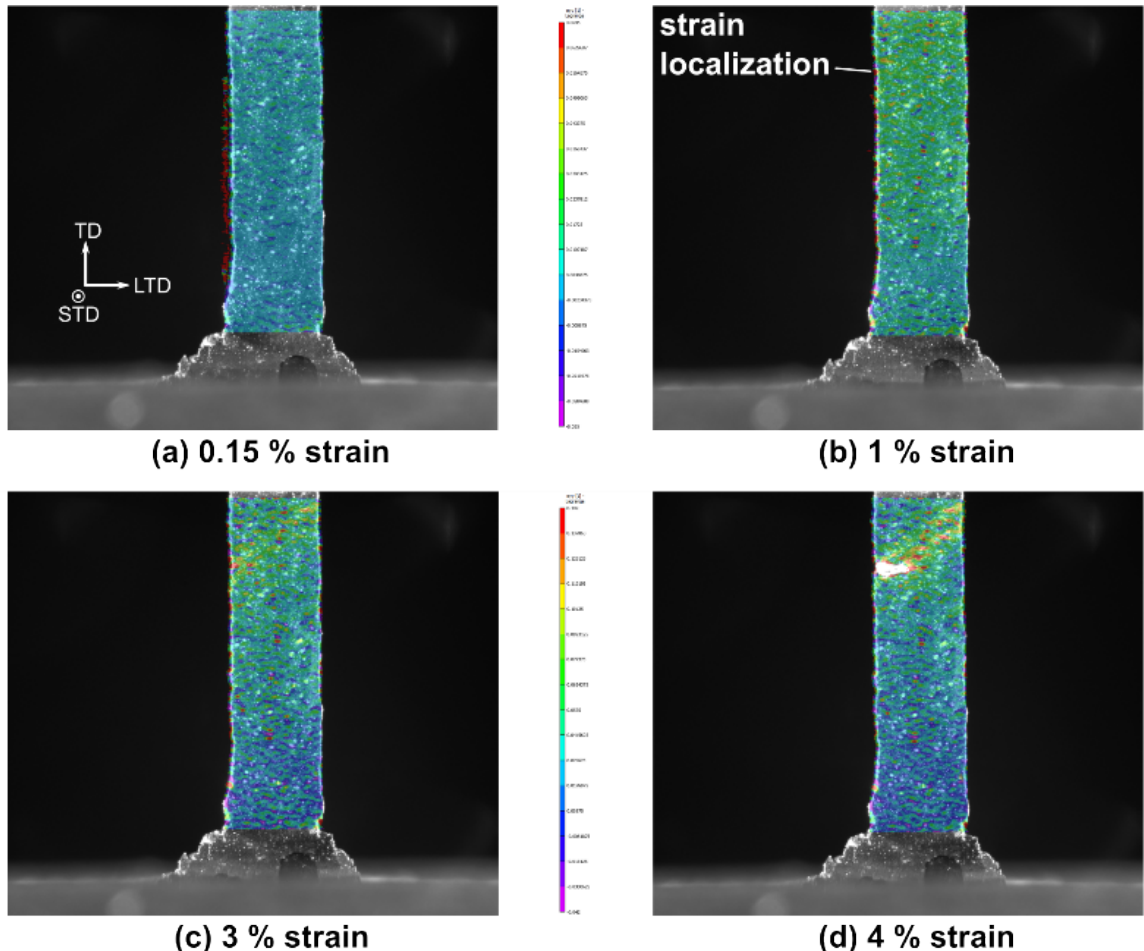
- Nano-indentation did not reveal any gradient in local strength from the edge to the interior of the material



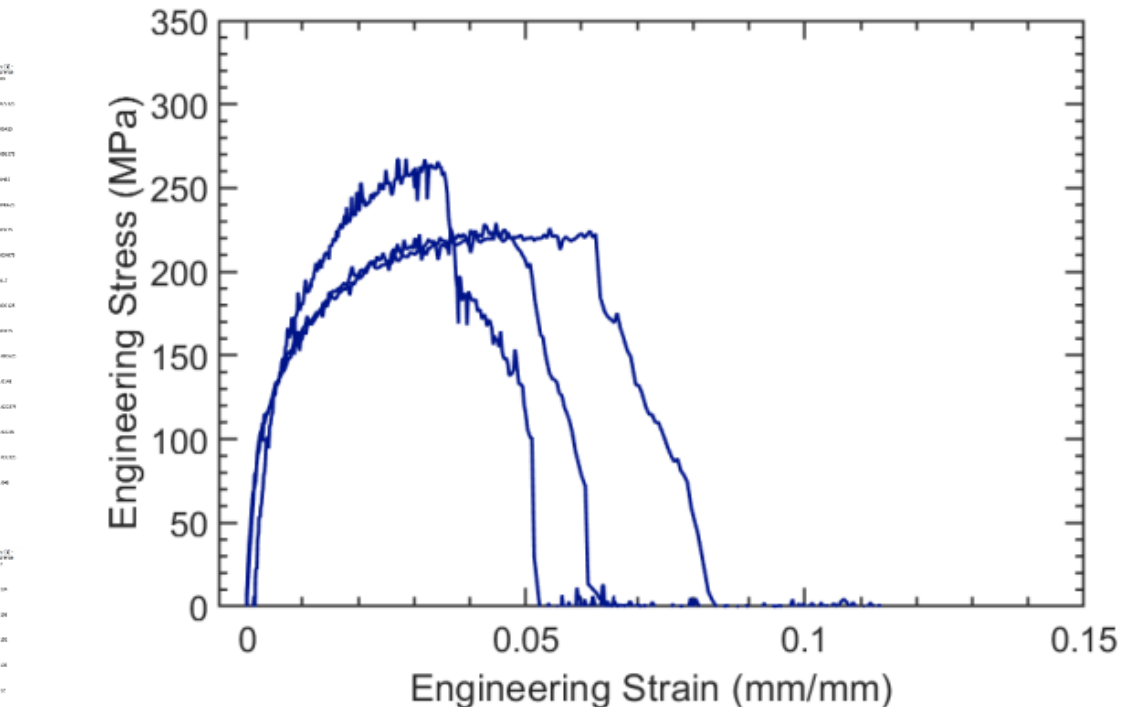
Stress-strain results from specimens thinned from one side are presented in Figure 16. Specimens with thicknesses of 600, 400, 200, and 100 μm are shown on the same plot and distinguished by color. The initial stress-strain behavior is similar between each test but the 400 μm specimens demonstrate slightly different initial slopes, although this may be attributed to test setup variability. As specimen thickness decreases, the strain to failure continually decreases; note that the specimen label 200 μm was actually thinner than the 100 μm specimen by a few microns. These test results demonstrate that ductility decreases significantly with decreasing thickness, which can be attributed to differences in mechanical properties and/or differences in defect content along the crust. Specimens demonstrate a similar stress-strain response with a consistent elastic modulus, but modulus is typically not a strong indicator of mechanical properties since it primarily depends on material chemistry. Additional mechanical properties such as UTS, ductility, and yield strength are stronger functions of thickness. The ACQ material tested has relatively few defects and demonstrates large differences in UTS, ductility, and yield strength. These results suggest that the crust does behave differently than the interior and this effect can be quantified. The precise cause of the reduced performance is likely attributed to surface defects and the texture variation along the crust increasing damage compared to material with the crust removed combined with a decrease in mechanical property values. The nature of how this failure initiates and progresses will be explored using the in-situ testing and specimens polished on both sides.



Mechanical Response



- DIC highlights strain localization along the edge material and formation of a elevated strain band
- Failure spreads from the exterior and across the sample along the strain band



Results from the RATMAM specimens thinned on both sides are presented in Figure 17; specimens were 660, 636, and 438 μm thick. The stress-strain response is similar to the ACQ large block specimens thinned from one side to 400 μm or less as shown in Figure 16. The variability between tests is likely caused by differences in thickness, with the thicker specimen capable of sustaining more load before initiating failure. The evolution of the strain field as measured from DIC for one of the specimens polished on both sides is provided in Figure 18; strain is shown progressing from 0.15 % strain to 4 % strain, at which point failure initiates. Failure initiates at a strain localization appearing early in the deformation along the exterior edge of the specimen where the crust remained. This localization is the precursor to failure that progresses along a line of high strain that develops at 3 % strain. For all specimens, failure always begins on the short-transverse side of the gage region and follows a high strain line within the specimen. It is suspected that the strain line forms in relation to internal porosity.

Build Parameters



Stress relief anneal both builds:
550 F for 2 hours

Vendor 1

Al	Cu	Fe	Mg	Mn	N	Ni	O	Pb	Si	Sn	Ti
89.57	0.01	0.07	0.3	0.01	0.01	0.01	0.05	0.01	9.78	0.01	0.01

LPBF Tool	SLM 280HL
Hatch Spacing	150 μm
Layer Thickness	30 μm
Laser Power	350 W
Raster Speed	1100 mm/s
Beam Diameter	76.3 μm

Powder size: ASTM B822
20um

Vendor 2

Al	Cu	Fe	Mg	Mn	N	Ni	O	Pb	Si	Sn	Ti
89.57	0.01	0.07	0.3	0.01	0.01	0.01	0.05	0.01	9.78	0.01	0.01

LPBF Tool	EOS M400-1
Hatch Spacing	150 μm
Layer Thickness	60 μm
Laser Power	370 W
Raster Speed	1150 mm/s
Beam Diameter	90 μm

Powder size: ASTM B822
44um - vol% = min 40, max 70
32um - vol% = min 20, max 50
20um - vol% = min 00, max 10



Outline

Motivation and Background

- Jay Carroll's work identified that the surface "crust" in AM Al-10Si-Mg influences mechanical performance
- They saw the crust and determined that it can degrade performance and increase variability, but didn't explore if that region exhibits fundamentally different properties than the interior region.
- Understanding the crust is important because it is unlikely you can always remove it from small or complex parts or if you plan to use AM in an "as-built" state. And if the crust is going to be included in a part, then we need to develop modeling or meshing capabilities that can account for the crust and the variability it may bring to a design.
- The
- We hypothesized that we ca

Project Goals

- Identify regional mechanical behavior in AM metals using microscale, in-situ techniques to inform models
- Determine fracture evolution with in-situ methods and observe deviations around defects and along the transitional region

Material

- Vendor 1 is ACQ material. Describe the build and where specimens were cut from
- Vendor 2 is CarTec material. Describe build and where specimens were cut from.

Microstructure

- Show microstructure of vendor 1 and vendor 2. Note the distinction between the surface and the interior.

Experimental Test Plan

- Base material used as the control

Results

Summary

Model Parameters



Following mesh generation, the mesh underwent simulated tensile loading using the Sierra/SolidMechanics finite element package [5]. The plastic response of the material was captured using Voce isotropic hardening:

$$\sigma = \sigma_y + A(1 - \exp(-n\epsilon_p))$$

where ϵ_p is the plastic strain, σ_y is the yield stress, A is the hardening constant, and n is the hardening exponent.

Damage was modeled by accounting for both void nucleation and void growth. Nucleation results in the production of new voids in the material. The void nucleation model takes a form similar to Horstemeyer and Gokhale [6].

$$\eta = \eta \epsilon_p N_3 p \sigma_e \#(2)$$

where p is the hydrostatic stress, σ_e is the equivalent stress, N_3 is the triaxiality constant, and η represents the number of voids per unit volume. Following void nucleation, void growth was modeled by the following equation developed by Cocks and Ashby [7]:

$$\phi = 23\epsilon_p - (1-\phi)m + 1(1-\phi)m \sinh 2(2m-1)2m + 1p \sigma_e \#(3)$$

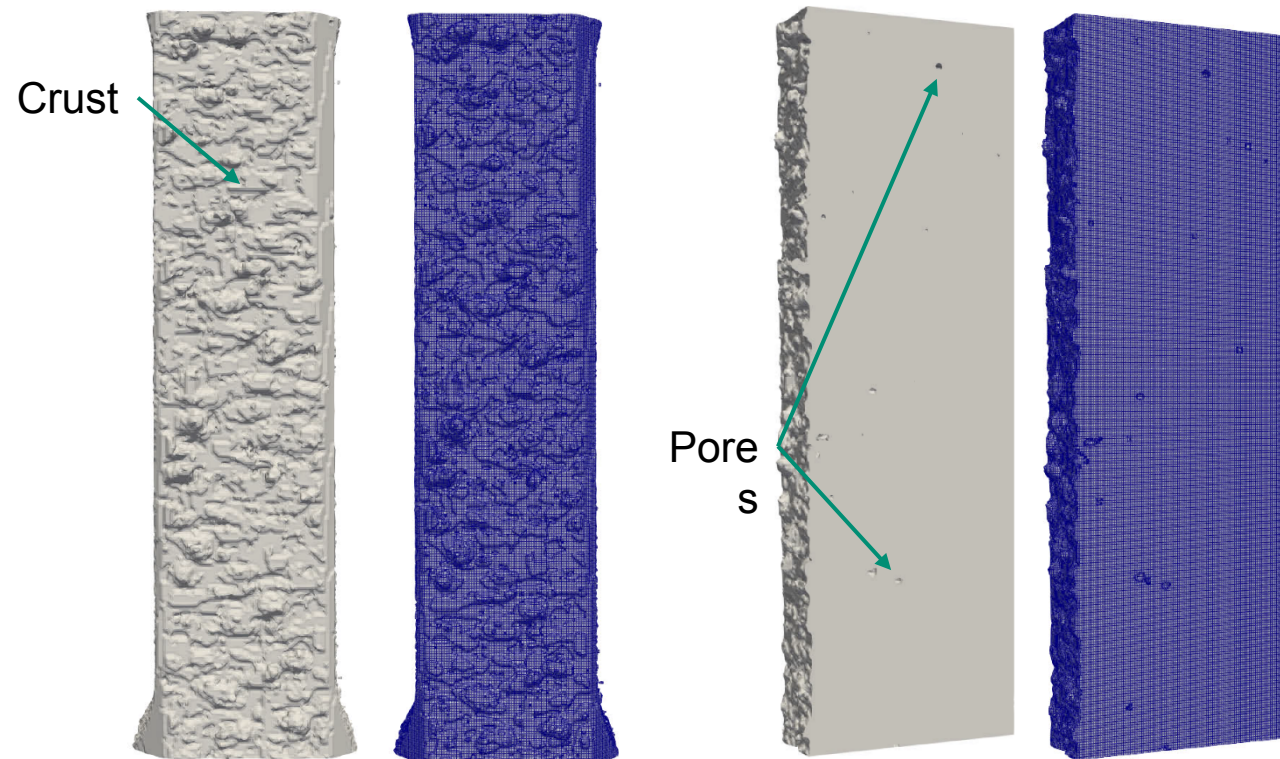
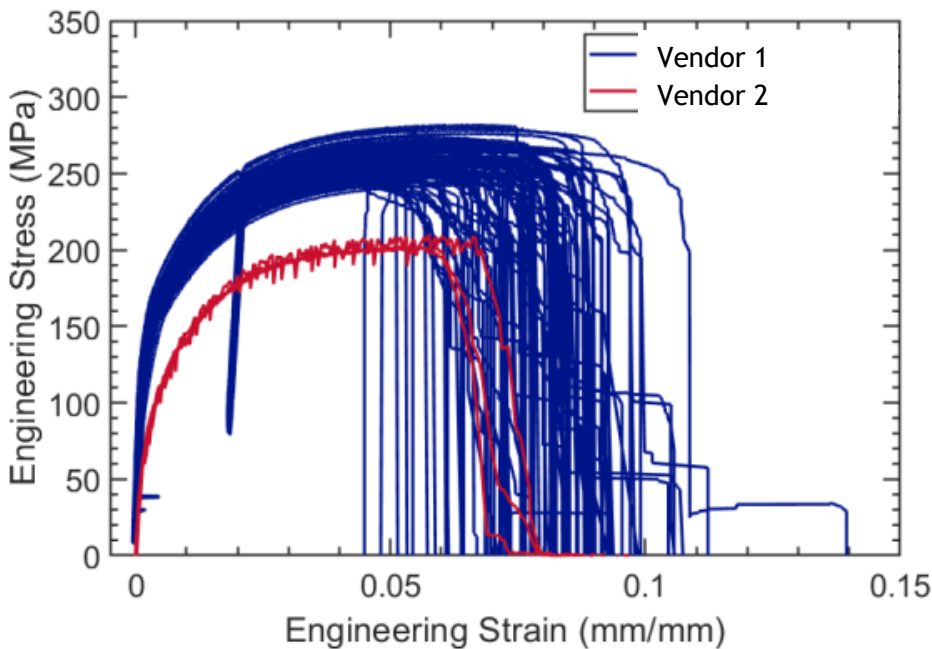
where ϕ is damage, and m is the damage exponent. These parameters were analytically calculated to high throughput as-printed tensile data initially, then further calibrated to the in-situ specimen response. The parameter values used in the study can be seen in *Table 5 below*.

Elastic Modulus, E	67.6 GPa
σ_y	138 MPa
A	180 MPa
n	20
m	3.5
N_3	2.0

High-fidelity Modeling



- Material model calibrated using full-size 1 mm dogbones
- Voce isotropic hardening
- Damage from void nucleation and growth
 - Based on Horstemeyer & Gokhale and Cocks & Ashby



Mesh of tensile specimen CT scan

- CT scan directly used to mesh geometry
- Direct numerical simulations (DNS) of these meshes paired with in situ tensile testing allows for comparison of edge, geometry, and pore effects